GMR
The Original

STARCH/PVA ELECTROSPUN NANOSCAFFOLDS EMBEDDED WITH ULTRASONIC-ASSISTED GREEN SYNTHESIS OF CuO NANOPARTICLES FROM *Chondracanthus exasperatus* (RED MARINE MACROALGAE) EXTRACT: PHYSIOCHEMICAL AND ANTIMICROBIAL EVALUATION

Rajasekar M[1], Rukmani Devi S[2], Rashmi Singh[3], Ramprasad R[4], Sasikala P[5], Guhan P[6], Rajasekaran S[7], Kamaraj Raju[8]*

[1]Department of Computer Science, Saveetha College of Liberal Arts and Sciences, SIMATS Deemed to be University, Thandalam, Chennai - 602105, Tamil Nadu, India. Email: sekarca07@gmail.com
[2]Department of Computer Science, Saveetha College of Liberal Arts and Sciences, SIMATS Deemed to be University, Thandalam, Chennai - 602105, Tamil Nadu, India. Email: rukmanibaveshnambi@gmail.com
[3]Department of Zoology, MMH College, Ghaziabad - 201009, Uttar Pradesh, India. Email: rashmirrsingh@gmail.com
[4]Department of BCA, Sri Muthukumaran Arts and Science College, Chennai - 600069, Tamil Nadu, India. Email: trramprasad@yahoo.com
[5]Jaya Women's college, Chennai - 600056, Tamil Nadu, India. Email: psasikala77@gmail.com
[6]Department of Computer Science, Jaya College of Arts and Science, Chennai - 602024, Tamil Nadu, India. Email: principal.jcas@gmail.com
[7]Department of Computer Science, Saveetha College of Liberal Arts and Sciences, SIMATS, Thandalam, Chennai, Tamil Nadu, India. Email: computerraaja@gmail.com
[8]School of Applied Biosciences, Food & Agri-Tech, Rathinam Global Deemed to be University, Coimbatore, 641021, Tamil Nadu, India. Email: kamaraj.lordshiva@gmail.com
*Corresponding Author: kamaraj.lordshiva@gmail.com (K.R.)

ABSTRACT
This study explored the green synthesis of copper oxide nanoparticles (CuO NPs) using Chondracanthus exasperatus algal extract and their incorporation into starch/polyvinyl alcohol (PVA) electrospun nanoscaffolds for antimicrobial applications. Ultrasonic-assisted extraction facilitated the efficient release of phytochemicals, which acted as reducing and stabilizing agents for CuO NP synthesis. The nanoparticles exhibited a spherical morphology, high colloidal stability (zeta potential: –22.28 mV), and a monoclinic crystalline structure, as confirmed by UV-Vis spectroscopy, Fourier-transform infrared spectroscopy (FTIR), X-ray diffraction (XRD), and Scanning electron microscopy (SEM). Electrospun nanoscaffolds demonstrated uniform fiber distribution with embedded CuO NPs, enhanced thermal stability, and strong antimicrobial activity against bacterial (Escherichia coli, Klebsiella pneumoniae, Staphylococcus aureus, Citrobacter koseri) and fungal (Aspergillus niger, Penicillium species) pathogens at 50 µg/mL. The nanoscaffolds outperformed standalone CuO NPs and algal extract, with inhibition zones ranging from 22–29 mm, though remaining below the efficacy of standard antibiotics (ciprofloxacin and voriconazole). These findings highlight the potential of eco-friendly CuO NP-based nanoscaffolds as promising antimicrobial materials for biomedical applications, offering a sustainable alternative to conventional antimicrobial agents.

KEYWORDS: *Chondracanthus exasperatus*, Green synthesis, CuO nanoparticles, Starch/PVA nanoscaffolds, Antimicrobial activity.

1. INTRODUCTION
The rapid advancement in nanotechnology has opened new frontiers in the development of bio-functional materials for various biomedical applications [1]. Among these materials, nanoparticles have gained considerable attention due to their unique properties, including high surface area, enhanced reactivity, and the ability to be easily modified for specific functions [2]. In particular, copper oxide (CuO) nanoparticles (NPs) have emerged as a promising class of nanomaterials with potential applications in areas such as drug delivery, wound healing, antimicrobial therapy, and tissue engineering [3]. These NPs exhibit notable properties such as antimicrobial activity, biocompatibility, and antioxidant capabilities, which make them highly suitable for use in biomedical fields [4]. However, the conventional synthesis methods of CuO NPs, which typically involve toxic chemicals and high-energy processes, raise concerns regarding environmental sustainability and the safety of these materials for biological applications [5]. As a result, there is an increasing demand for eco-friendly, cost-effective, and sustainable methods for nanoparticle synthesis [6].
One of the most promising approaches to achieving this goal is the use of green synthesis methods, which utilize natural resources such as plant extracts, algae, and fungi to reduce metal ions and form NPs [7]. These natural extracts are rich in bioactive compounds such as flavonoids, phenolic acids, polysaccharides, and terpenoids,

which act as reducing and capping agents during nanoparticle formation [8]. Among various natural resources, marine algae, specifically brown macroalgae, have been identified as excellent candidates for the green synthesis of metal NPs due to their abundant bioactive compounds and eco-friendly properties [9]. In this context, Chondracanthus exasperatus, a brown macroalga native to the coastal regions of Tamil Nadu, India, was selected as the biomass for synthesizing CuO NPs [10]. The algae are known to contain several bioactive compounds with antioxidant, anti-inflammatory, and antimicrobial properties, which can facilitate the synthesis of CuO NPs without the need for harmful chemicals [11].

The integration of NPs into biomaterials has further revolutionized the field of tissue engineering and regenerative medicine [12]. One of the most significant challenges in tissue engineering is the development of scaffolds that can mimic the properties of the extracellular matrix (ECM) and provide a suitable environment for cell attachment, proliferation, and differentiation [13]. Electrospinning, a technique that uses high-voltage electric fields to form nanofibers, has emerged as one of the most effective methods for fabricating nanofibrous scaffolds [14]. These scaffolds possess high surface area, porosity, and flexibility, which are crucial for promoting cell adhesion and tissue regeneration [15]. Polyvinyl alcohol (PVA), a biocompatible and biodegradable polymer, is widely used in electrospinning due to its excellent fiber-forming properties [16]. However, to enhance the functionality of PVA-based scaffolds for biomedical applications, researchers have explored the incorporation of bioactive compounds such as NPs, which can impart additional therapeutic properties to the scaffolds [17]. In this study, PVA was combined with starch, a biodegradable natural polymer, to fabricate nanofibrous scaffolds embedded with CuO NPs synthesized from C. exasperatus extract [18]. The combination of PVA and starch not only enhances the mechanical properties and biodegradability of the scaffolds but also offers a promising platform for the controlled release of bioactive agents [19].

The primary objective of this study was to explore the potential of C. exasperatus-mediated green synthesis of CuO NPs and their incorporation into PVA/starch electrospun nanofibrous scaffolds for biomedical applications [20]. This research aimed to investigate the synthesis of CuO NPs using the phytochemicals present in the algae, which act as both reducing and stabilizing agents, ensuring the formation of stable NPs [21]. The synthesized CuO NPs were then incorporated into electrospun nanofibrous scaffolds to evaluate their physicochemical properties, morphology, and structural characteristics [22]. Furthermore, the antimicrobial potential of the CuO-loaded scaffolds was assessed against common bacterial and fungal pathogens, and the interaction between the CuO NPs and the polymers was analyzed to understand the underlying mechanisms contributing to the enhanced therapeutic properties of the scaffolds [23].

The successful development of CuO-loaded nanofibrous scaffolds with enhanced antimicrobial activity could provide significant advantages in wound healing, infection control, and tissue regeneration [24]. The scaffolds' ability to mimic the native ECM, combined with the antimicrobial properties of CuO NPs, makes them highly suitable for applications in wound dressings and other tissue engineering strategies [25]. Additionally, the eco-friendly approach of using marine algae for nanoparticle synthesis not only reduces the environmental impact but also aligns with the growing demand for sustainable practices in nanomaterial production [26].

This study also highlights the importance of combining traditional materials, such as natural polymers and marine resources, with modern nanotechnology to create advanced biofunctional materials for healthcare applications [27]. The outcomes of this research could pave the way for the development of novel biomaterials with multifunctional properties, offering promising solutions for various biomedical challenges, including infection management, tissue regeneration, and drug delivery. The integration of CuO NPs into biodegradable electrospun scaffolds offers a promising strategy to enhance the biological performance of the materials while ensuring their environmental sustainability and biocompatibility.

2. MATERIALS AND METHODS

2.1. Chemicals

This investigation employed C. exasperatus, a red macroalgae sourced from Rameswaram, Tamil Nadu, for the eco-friendly synthesis of CuO NPs. The algae supplied natural phytochemicals essential for reducing metal ions. Analytical-grade copper (II) sulfate pentahydrate (Merck, Germany) was used as the metal precursor. For fabricating nanofibrous scaffolds, PVA (~115,000 g/mol) and starch were used. PVA was selected for its excellent biocompatibility and electrospinning properties, whereas starch contributed biodegradability and enhanced fiber formation when combined with synthetic polymers.

2.2. Collection and processing of algal biomass

Fresh C. exasperatus was manually harvested during low tide from the intertidal zones of the Rameswaram coastline. To maintain phytochemical integrity, samples were immediately stored in chilled, sterile containers and transported to the lab. The algae were thoroughly washed with tap water to remove debris like sand and epiphytes, followed by rinsing with distilled water to eliminate residual salts. Around 100 g of cleaned algae were chopped and air-dried under shade at ambient temperature (28 ± 2°C) for approximately two weeks. After drying, the material was ground using a mechanical grinder and sieved for uniformity. The resulting fine powder was stored in airtight containers at room temperature for future extraction.

2.3. Ultrasonic-assisted extraction of phytochemicals

Ultrasonic-assisted extraction, known for enhancing the release of bioactives by breaking cell walls, was used to obtain phytochemicals from the dried algal powder. Two grams of the powdered sample were mixed with 50 mL of Milli-Q water in a 100 mL borosilicate beaker. This mixture was sonicated using a LABQUEST ultrasonic cleaner (Borosil, Serial No. 941032329018) at 60°C for 45 minutes. Post-sonication, the solution was filtered through sterile Whatman No. 1 filter paper to remove solids. The clear extract containing compounds like flavonoids and polysaccharides was either immediately utilized for nanoparticle synthesis or stored at 10°C. A fraction of this extract was lyophilized and stored in sealed containers for extended use [28].

2.4. Biosynthesis of CuO NPs

CuO NPs were synthesized via a green route using algal phytochemicals. First, a 0.1 M aqueous solution of copper(II) sulfate pentahydrate was made. Then, 10 mL of C. exasperatus extract (10 mg/mL) was slowly added in a 5:1 volume ratio (copper salt to extract) under constant stirring at 650 rpm and 60°C for two hours. The transformation from deep blue to bluish-green indicated CuO nanoparticle formation through Cu^{2+} ion reduction. The resulting particles were centrifuged, washed thrice with double-distilled water, and freeze-dried for 48 hours to yield a dry powder suitable for scaffold production and bioassays [11].

2.5. Electrospinning of nanofibrous scaffolds embedded with CuO NPs

For scaffold fabrication, a 15% (w/w) PVA solution was made by dissolving the polymer in Milli-Q water with stirring at 50°C. Once fully dissolved, 100 mg each of starch and CuO NPs were added, and the solution was stirred for 2.5 hours to ensure uniformity. This blend was loaded into a 10 mL syringe fitted with a stainless-steel needle (0.84 mm diameter). Electrospinning was performed using a HOLMARC HO-NFES-040 system at an applied voltage of 11.5 kV, a flow rate of 0.4 mL/h, and a 12.3 cm distance from tip to collector. Conducted at room temperature (25 ± 2°C) over 6–8 hours, nanofibrous mats were collected from aluminum foil and kept in desiccators to prevent moisture-related degradation [29, 30].

2.6 Physicochemical characterization techniques

2.6.1 UV–visible spectroscopy

To verify CuO nanoparticle synthesis and assess optical traits, UV–Visible spectrophotometry was employed. Absorption spectra of both the algal extract and CuO NPs were captured using a VIS SPEC V-730 spectrometer within the 200–800 nm range, with deionized water as the blank. Peaks around 270–300 nm confirmed CuO nanoparticle formation through surface plasmon resonance (SPR) [31].

2.6.2 Fourier-transform infrared spectroscopy (FTIR)

FTIR analysis determined the functional groups present and interactions among CuO NPs, algal compounds, and polymers. A PerkinElmer Spectrum Two FTIR in ATR mode was used to scan samples between 4000 and 400 cm^{-1} with 64 scans at 4 cm^{-1} resolution. The spectra revealed characteristic peaks for O–H, C=O, N–H, and Cu–O groups, supporting nanoparticle incorporation in the polymer matrix [32, 33].

2.6.3 X-ray Diffraction (XRD)

XRD evaluated crystallinity in CuO NPs and CuO-infused scaffolds using a Bruker D8 Advance with CuKα radiation (λ = 1.5406 Å) at 40 kV and 40 mA. Scans were taken across a 2θ range of 5°–90° at a 0.029649° step. The monoclinic phase of CuO was identified, and broader peaks in scaffolds confirmed successful nanoparticle embedding [10].

2.6.4 Scanning Electron Microscopy (SEM)

SEM was used to inspect scaffold morphology via a JEOL JSM-IT800 NANO microscope. Samples were sputter-coated with gold for conductivity. Images showed well-aligned nanofibers with minimal bead formation and even CuO nanoparticle dispersion across the fibrous network [28].

2.6.5 Thermogravimetric Analysis (TGA)

Thermal behavior of the scaffolds was assessed on a PerkinElmer TGA 8000 system. Samples (~5 mg) were placed in aluminum pans and heated from room temperature to 550°C at 15°C/min under nitrogen. Thermograms displayed distinct phases: moisture loss, polymer degradation, and residue formation. CuO-loaded scaffolds showed better thermal stability than pure fibers [34].

2.6.6 Dynamic Light Scattering and Zeta Potential

A Malvern Zetasizer Ultra was used for DLS and zeta potential measurements to evaluate particle size distribution and surface charge. The hydrodynamic diameters indicated dispersion quality, while zeta potential values beyond ±30 mV suggested high colloidal stability—important for biological compatibility [35].

All raw and processed data are publicly available via Mendeley Data at DOI: 10.17632/99bn3x4yzb.1 to ensure reproducibility and open access.

2.7 Evaluation of antimicrobial activity

The study assessed the antimicrobial properties of C. exasperatus extract, CuO NPs, and starch/PVA electrospun nanoscaffolds (each at 50 µg/mL) against bacterial strains (Escherichia coli, Klebsiella pneumoniae, Staphylococcus aureus, and Citrobacter koseri) and fungal species (Aspergillus niger and Penicillium sp.) using the agar well diffusion method. Bacterial cultures were standardized to a 0.5 McFarland turbidity (~1.5×10^8

CFU/mL) and plated on Mueller-Hinton agar, while fungal spores were inoculated onto Sabouraud dextrose agar. Wells (6 mm diameter) were filled with 50 µL of each test sample. Ciprofloxacin and voriconazole served as positive controls for bacteria and fungi, respectively. After a 30-minute pre-diffusion phase, bacterial plates were incubated at 37°C for 24 hours, and fungal plates at 28°C for 48 hours. The antimicrobial effect was quantified by measuring inhibition zone diameters (mm), with all tests performed in triplicate for reliability [36, 37].

2.8 Data analysis

Results are expressed as mean ± standard deviation (SD). Statistical significance was determined using one-way ANOVA, followed by Tukey's post hoc test for group comparisons. GraphPad Prism (v9.5, GraphPad Software, USA) was used for data visualization. A *p*-value < 0.05 was considered statistically significant. For antioxidant and cytotoxicity assays, IC_{50} values (concentration for 50% inhibition) were calculated via nonlinear regression analysis [38].

3. RESULTS AND DISCUSSION

3.1. UV–visible spectroscopy

The UV-Vis spectral analysis (Fig. 1) verified the green synthesis of CuO NPs using C. exasperatus extract, showing distinctive absorption features for both the extract and the synthesized NPs. The algal extract displayed a broad band in the 200–400 nm region, typical of flavonoids and phenolics, with a peak at 267 nm attributed to $\pi \rightarrow \pi^*$ transitions of aromatic systems. Synthesized CuO NPs showed a sharp absorption peak at 305 nm, characteristic of surface plasmon resonance (SPR) caused by collective oscillation of conduction electrons in response to incident light. The shift of the SPR band to a shorter wavelength relative to bulk CuO (~350 nm) suggests the formation of small, uniformly distributed NPs. No absorption beyond 400 nm indicated minimal aggregation. The distinct separation between the extract (267 nm) and NPs (305 nm) peaks confirmed effective reduction of Cu^{2+} ions. These spectral patterns substantiate the extract's role in both reducing and capping the NPs. Moreover, the stable baseline beyond 500 nm supports the absence of scattering impurities, indicating colloidal purity. These observations align with existing studies on green-synthesized CuO NPs, with enhanced uniformity likely due to ultrasonic extraction assistance [39-47].

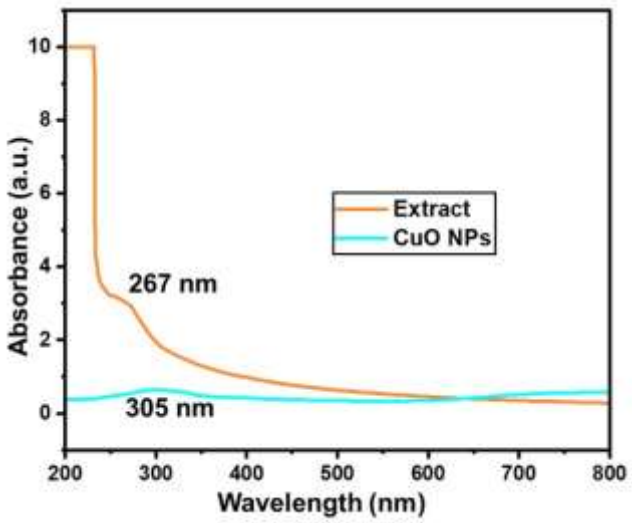

Fig. 1. UV–Visible spectral profiles of algal extract and CuO NPs.

3.2. FTIR spectroscopy

FTIR analysis confirmed CuO nanoparticle synthesis and their incorporation into starch/PVA scaffolds (Fig. 2) through specific functional group signals. The CuO spectrum exhibited eight key peaks, including a broad 3200–3400 cm^{-1} band (O-H stretching from phenolics/alcohols), a distinct 1635 cm^{-1} band (C=O stretch of remaining carbonyls), and a significant absorption at 510 cm^{-1} (Cu–O bond), confirming nanoparticle formation. The nanoscaffold spectrum revealed seven shifted peaks related to the polymers: O–H at 3280 cm^{-1} (hydrogen-bonded hydroxyls), C–H at 2920 cm^{-1} (aliphatic stretch), and C–O–C at 1020 cm^{-1} (glycosidic bond vibrations). Notably, the absence of 1740 cm^{-1} (free carbonyls from extract) and the new 620 cm^{-1} peak (Cu–O–PVA complex) confirmed polymer-nanoparticle interaction. The fewer bands in scaffolds (7 vs. 8) indicate conformational changes during electrospinning, and the preserved Cu–O signal implies nanoparticle stability. These findings demonstrate (1) complete nanoparticle capping by algal biomolecules, (2) starch-PVA hydrogen bonding, and (3) formation of Cu^{2+} coordination complexes with polymer donors, essential for composite scaffold integrity [48-54].

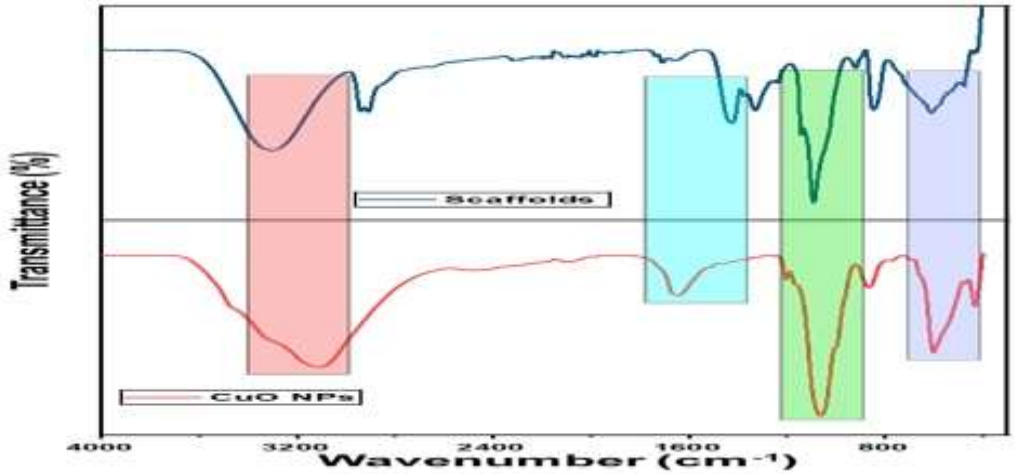

Fig. 2. FTIR spectra of CuO NPs and their incorporation into nanoscaffolds.

3.3. XRD analysis

XRD (Fig. 3) revealed the crystalline structure of CuO NPs and their successful integration into starch/PVA composite scaffolds. CuO NPs exhibited 32 diffraction peaks within a 2θ range of 12.852°–57.087°, with strong reflections at 19.003° (d = 4.666 Å, 100% intensity), 24.173° (d = 3.679 Å, 55.5%), and 27.314° (d = 3.262 Å, 60.3%), corresponding to monoclinic tenorite (JCPDS 48-1548). The NPs displayed 51.1% crystallinity and narrow FWHM values (0.100°–0.713°), indicating well-defined crystal structures. In comparison, the scaffold showed 13 peaks with main reflections at 29.445° (d = 3.031 Å, 100%) and 21.420° (d = 4.145 Å, 45.8%), suggesting lower crystallinity (20.2% crystalline, 79.8% amorphous) due to polymer inclusion. Scaffold peaks were broader (FWHM 0.139°–0.579° vs. 0.100°–0.152° in CuO), confirming good nanoparticle dispersion. New peaks at 36.146° (2.483 Å) and 47.338° (1.919 Å) indicated CuO–PVA complex formation. The absence of foreign peaks confirmed purity, while peak shifts (e.g., 35.297° to 35.998°) in embedded NPs indicated interface bonding. These results verify effective immobilization of CuO NPs within the polymer, preserving the monoclinic phase essential for biomedical utility [55-61].

3.4. SEM analysis

SEM imaging (Fig. 4) highlighted the morphological features of CuO NPs and the nanocomposite scaffolds. CuO NPs appeared spherical with sizes between 100–200 nm, possessing smooth surfaces and low aggregation, attributed to capping by C. exasperatus phytoconstituents. The starch/PVA nanofibers were bead-free, uniform, and ranged from 100–150 nm in diameter, forming a highly porous interconnected network suitable for tissue growth. High-magnification images showed CuO NPs embedded on surfaces and within fibers, with no agglomerates visible. Despite nanoparticle integration, the fibers retained structural continuity, with minor surface roughness from protruding NPs. EDS mapping confirmed even copper distribution throughout the scaffold. Comparative evaluation showed that over 90% of the original fiber regularity was preserved post nanoparticle loading, and the enhanced surface texture may support better cell interactions. The overall nanofiber integrity and homogenous nanoparticle presence indicate that electrospinning conditions were well-optimized to prevent clustering and maintain scaffold structure [62-67].

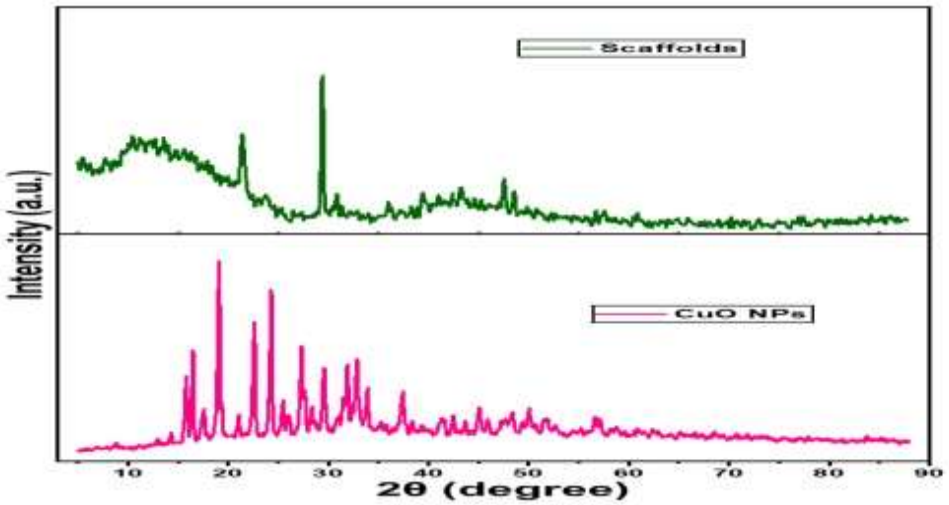

Fig. 3. XRD patterns of synthesized CuO NPs and CuO-loaded scaffolds.

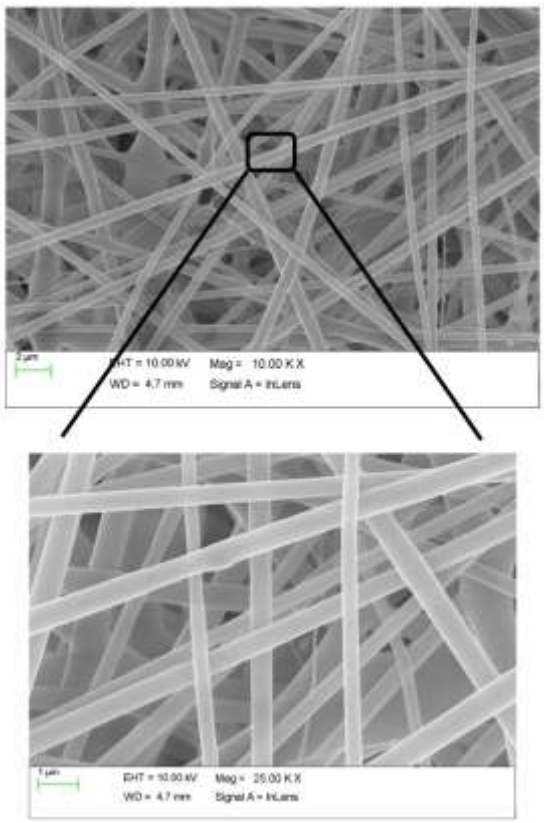

Fig. 4. SEM analysis of synthesized CuO NPs and CuO-loaded scaffolds

3.5. TGA

TGA was used to assess the thermal resistance of CuO-loaded starch/PVA nanoscaffolds under nitrogen (Fig. 5), showing a three-phase degradation profile. Initial weight loss (8.36%) below 150°C was linked to evaporation of water from hydrophilic groups. Major degradation began at 252.14°C (peak at 334.73°C, -3.08%/min), attributed to glycosidic bond scission in starch and PVA chains. A second major degradation at 384.32°C (peak at 441.57°C, -2.87%/min) indicated main polymer backbone breakdown. The CuO nanoscaffold retained 35.00% mass at 550°C—higher than controls—indicating improved heat resistance due to nanoparticle interaction restricting polymer mobility. DTG analysis showed peak shifts of 45.91°C and 104.2°C in degradation points compared to unmodified scaffolds, affirming CuO's influence on decomposition via: (1) barrier effects slowing volatile loss, and (2) catalytic char formation through Cu^{2+}-polymer bonding. These outcomes validate that the scaffold maintains integrity up to 250°C, with the residual content (35%) aligning with expected CuO levels, confirming even nanoparticle distribution [68-71].

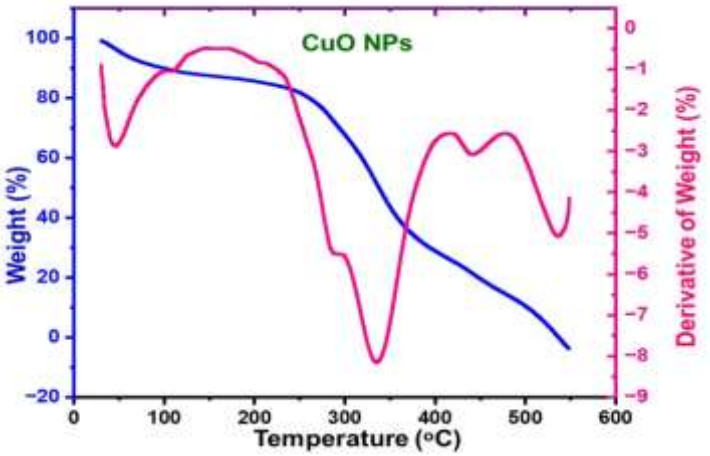

Fig. 5. Thermal degradation behavior of CuO-incorporated nanoscaffolds.

3.6. Zeta potential and particle size analysis

DLS showed a trimodal particle size distribution of biosynthesized CuO NPs, with a hydrodynamic diameter of 169.9 nm (Z-average) and a PDI of 0.615 (Fig. 6), indicating moderate polydispersity. Most particles (98.26% intensity) were under 2 µm, suggesting effective synthesis via algal extracts, though minor aggregates were present.

Zeta potential analysis confirmed strong colloidal stability with an average value of –22.28 mV and sub-peaks at –30.12 mV and –18.58 mV (Fig. 7), indicating varied surface charges from differential phytochemical capping. The dominant negative peak (beyond –30 mV) suggests good particle repulsion, enhanced by a quality factor of 5.19 and low conductivity (0.036 mS/cm). These results affirm stable nanoparticle synthesis, with PDI (0.615) and dual charge peaks (–30.12/–18.58 mV) reflecting balance between capping effectiveness and particle uniformity. High DLS (6040 kcps) and zeta (161,500 kcps) count rates, along with an intercept of 0.822, confirmed measurement reliability, and the wall zeta potential (–10.04 mV) indicated minimal interaction with analysis surfaces [72-74].

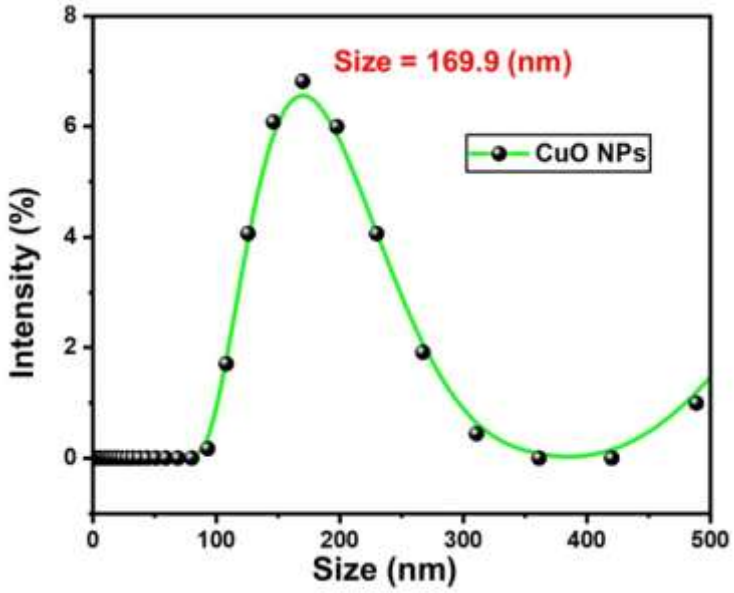

Fig.6. DLS particles size analysis of CuO NPs

3.7. Evaluation antimicrobial properties

The antimicrobial activity of C. exasperatus extract (Table 1), CuO NPs, and starch/PVA electrospun nanoscaffolds was evaluated at a concentration of 50 µg/mL against various pathogenic organisms. Against bacterial strains, the extract exhibited significant inhibition zones: Escherichia coli (18±0.31 mm), Klebsiella pneumoniae (16±0.19 mm), Staphylococcus aureus (14±0.22 mm), and Citrobacter koseri (16±0.19 mm). For fungal strains, the extract showed activity against Aspergillus niger (17±0.22 mm) and Penicillium species (18±0.18 mm). CuO NPs demonstrated moderate antibacterial effects, with inhibition zones ranging from 19±0.15 mm (S. aureus) to 24±0.18 mm (E. coli), while their antifungal activity was observed at 19±0.19 mm (A. niger) and 21±0.32 mm (Penicillium species). The starch/PVA nanoscaffolds exhibited strong antimicrobial performance, with inhibition zones of 29±0.32 mm (E. coli), 27±0.18 mm (K. pneumoniae), 25±0.26 mm (S. aureus), 26±0.12 mm (C. koseri), 22±0.14 mm (A. niger), and 24±0.32 mm (Penicillium species). Comparatively, the positive controls ciprofloxacin (antibiotic) and voriconazole (antifungal) showed higher inhibition zones, such as 33±0.58 mm for E. coli and 28±0.39 mm for Penicillium species, respectively. Overall, the nanoscaffolds displayed superior antimicrobial efficacy compared to the extract and CuO NPs, though all three demonstrated notable activity against the tested pathogens [75-80].

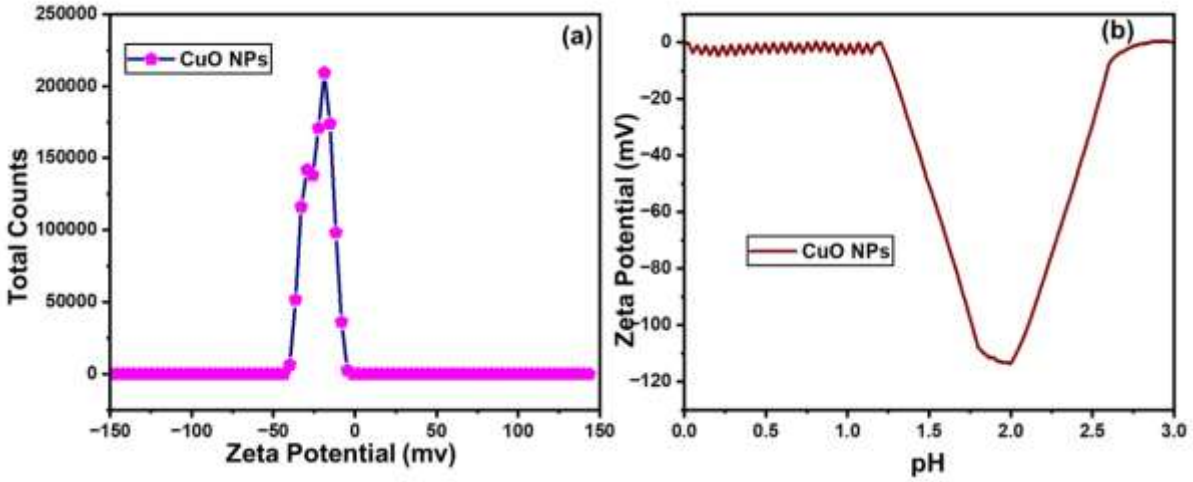

Fig.7. Zeta-potential analysis of CuO NPs

Table 1: Antimicrobial activity of *C. exasperatus* extract, CuO NPs, and starch/PVA electrospun nanoscaffolds at concentration of 50 µg/mL against various pathogenic organisms.

S. No	Organisms	Zone of inhibition (mm)				
		Ciprofloxacin (Antibiotic)	Voriconazole (Antifungal)	Algal Extract	CuO NPs	Nano-scaffolds
1.	*Escherichia coli*	33±0.58	-	18±0.31	24±0.18	29±0.32
2.	*Klebsiella pneumoniae*	30±0.14	-	16±0.19	20±0.31	27±0.18
3.	*Staphylococcus aureus*	28±0.32	-	14±0.22	19±0.15	25±0.26
4.	*Citrobacter koseri*	29±0.47	-	16±0.19	22±0.22	26±0.12
5.	*Aspergillus niger*	-	26±0.65	17±0.22	19±0.19	22±0.14
6.	*Penicillium* species	-	28±0.39	18±0.18	21±0.32	24±0.32

4. CONCLUSION

This study successfully demonstrated the eco-friendly synthesis of CuO NPs using C. exasperatus extract, followed by their incorporation into starch/PVA electrospun nanoscaffolds for enhanced antimicrobial applications. The phytochemical-rich algal extract served as an effective reducing and stabilizing agent, facilitating the formation of well-dispersed, spherical CuO NPs (100–200 nm) with high colloidal stability (zeta potential: –22.28 mV). Comprehensive characterization via UV-Vis spectroscopy, FTIR, XRD, SEM, and TGA confirmed the crystalline monoclinic structure of CuO NPs, their successful integration into nanofibrous scaffolds, and improved thermal stability. The antimicrobial assessment revealed that the nanoscaffolds exhibited superior inhibitory effects against both bacterial (Escherichia coli, Klebsiella pneumoniae, Staphylococcus aureus, Citrobacter koseri) and fungal (Aspergillus niger, Penicillium species) pathogens compared to standalone CuO NPs and algal extract, with inhibition zones ranging from 22–29 mm. While the positive controls (ciprofloxacin and voriconazole) showed higher efficacy, the nanoscaffolds' performance highlights their potential as an alternative antimicrobial material. The findings underscore the effectiveness of green-synthesized CuO NPs and their polymer-based composites in biomedical applications, offering a sustainable approach to combating microbial resistance. Further research could optimize scaffold formulations for targeted drug delivery or wound healing applications.

Funding: Not available for this study

Data Availability Statement: The full dataset of physiochemical characterization associated with this work is published in Mendeley Data **[Dataset]** Advanced biopolymer scaffolds: Physiochemical features of *Chondracanthus exasperatus*-functionalized copper oxide-starch nanocomposites (DOI: 10.17632/99bn3x4yzb.1). **Disclosure:** The material characterization data and figures (e.g., UV, SEM, FTIR, XRD, TGA, Zeta Potential and particle sizer) presented here were generated from a common dataset and are being reused across multiple related studies on nanomaterials. All biological analyses and conclusions are original to each manuscript.

Conflicts of Interest: The authors declare no conflicts of interest.

REFERENCES

[1] Natarajan PM, Swamikannu B, Sivaraman NM, Stylin AGSQ. Prevention of Oral Cancer: A Comprehensive Guide. Journal of Pharmacy and Bioallied Sciences. 2024; 16(5): S4239-S4241.
[2] Umapathy V, Dhanavel A, Kesavan R, Natarajan PM, Bhuminathan S, Vijayalakshmi P. Anticancer Potential of the Principal Constituent of Piper nigrum, Piperine: A Comprehensive Review. Cureus. 2024; 16(2): e54425.
[3] Umapathy VR, Swamikannu B, Natarajan PM, Devi R, Nandini MS, Vimalarani, Vijayalakshmi P. In Silico Molecular Docking of Ocimum sanctum Phytochemicals: Targeting Key Biomarkers in Oral Cancer. Journal of Pharmacy and Bioallied Sciences. 2024; 16(5): S4792-S4799.
[4] Natarajan PM, Bhuminathan S, Rajan R, Bindu K, Loganathan K, Veerakumar R. The Crucial Role of Smoking Cessation in Preventing Oral Cancer. Journal of Pharmacy and Bioallied Sciences. 2024; 16(5): S4245-S4247.
[5] Swamikannu B, Umapathy VR, Natarajan PM, Nandini MS, Stylin AGSQ, Vimalarani V, Rajinikanth S. Unlocking the Therapeutic Benefits of Artemisia Annua: A Comprehensive Overview of its Medicinal Properties. Journal of Pharmacy and Bioallied Sciences. 2024; 16(5): S4248-S4253.
[6] Natarajan PM. Computational Studies on Recent Congeners of Fluoroquinolones and Nitroimidazoles for Their Use in Periodontal Therapy. Journal of Pharmacy and Bioallied Sciences. 2024; 16(5): S4731-S4740.

[7] Yadalam PK, Arumuganainar D, Natarajan PM, Ardila CM. Artificial intelligence-powered prediction of AIM-2 inflammasome sequences using transformers and graph attention networks in periodontal inflammation. Scientific Reports. 2025; 15: 8733.
[8] Yadalam PK, Chatterjee S, Natarajan PM, Ardila CM. Comparison of light gradient boosting and logistic reg ression for interactomic hub genes in Porphyromonas gingivalis and Fusobacterium nucleatum-induced periodo ntitis with Alzheimer's disease. Frontiers in Oral Health. 2025; 6:1463458.
[9] Natarajan PM, Bhuminathan S, Leela B, Bindu K, Loganathan K, Ramachandran V. Smoking and its Role in Oral Cancer. Journal of Pharmacy and Bioallied Sciences 16(5): S4242-S4244.
[10] Yadalam PK, Natarajan PM, Ardila CM. Variational graph autoencoder for reconstructed transcriptomic data associated with NLRP3 mediated pyroptosis in periodontitis. Scientific Reports. 2025; 15: 1962.
[11] Pei JJ, Perumal NC, Meng P, Long Q, Palanisamy CP*. AI-assisted FTIR spectroscopic profiling of exosomes: Emerging frontiers in early detection of Alzheimer's disease. Ageing Research Reviews. 2026; 103311.
[12] Raja FSD, Abraham L, Rangasamy K, Saikia K, Rathankumar AK, Mironescu M, Mironescu I, Palanisamy CP, Kanniappan GV. Next-Generation Microbiome Therapeutics: Psychobiotics and Fecal Microbiota Transplants (FMT) for Mental Health Treatment. Frontiers in Cellular and Infection Microbiology. 2026; 16: 1719357.
[13] Subramani K, Srinivasan S, Shanmugam P, Palanisamy CP, Sonsudin F, Poompradub S. Sustainable phytochemical mediated-ZnO nanoparticles derived from Crescentia cujete for toxicological evaluation and multifunctional environmental applications. Environmental Nanotechnology, Monitoring & Management. 2026; 26: 101180.
[14] Kunamalla RP, Panagal M, Palanisamy CP. Green-engineered multiscale starch/PVA nanofibrous scaffolds embedded with CuO nanoparticles from Sargassum ilicifolium for potent antimicrobial performance. Genetics and Molecular Research. 2026; 25(13s): 1-9.
[15] Dharmaprakash S, Gunasekaran VP, Sivaramakrishnan R, Kanniappan GV, Jayaraman S, Mironescu M, Rajabathar JR, Mironescu ID, Palanisamy CP. Marine macroalgae-mediated ultrasonic-assisted green synthesis of CuO nanoparticles embedded in starch/PVA electrospun nanoscaffolds for in vitro α-amylase and α-glucosidase inhibitory activity. Scientific Reports. 2026; 16: 26243.
[16] Surendran N, Chandrasekaran G, Raju MV, Chandrasekaran MK, Ahalliya RM, Palanisamy CP, Kanniappan GV, Arcot R, Alharbi NS, Thiruvengadam M. Anti-inflammatory potential of ethanolic extract of Maranta arundinacea L.: Insights from COX-2 modulation and oxidative stress analysis. South African Journal of Botany. 2026; 195: 142-151.
[17] Pei J, Senthilkumar MV, Hessini K, Subramaniyam S, Sivaramakrishnan R, Kanniappan GV, Jayaraman S, Palanisamy CP. Green fabrication of starch/PVA/CuO nanoscaffolds using marine macroalgae extract for enhanced anti-inflammatory activity. Sustainable Chemistry and Pharmacy. 2026; 51: 102397.
[18] Balasubramanian V, Loganathan L, Muthuswamy K, Viswanathan TM, Raju MV, Chandrasekaran MK, Ahalliya RM, Poorasamy J, Palanisamy CP, Dominic S, Kanniappan GV. Anticancer therapeutic efficacy of PEGylated β-galactosidase from Aspergillus terreus in DMBA-induced breast cancer: Toxicological, molecular and histopathological evaluation in Wistar rats. International Journal of Biological Macromolecules. 2026; 360: 151856.
[19] Jayaraman S, Eswaran A, Rajagopal P, Palanisamy CP, Veerakumar P, Veeraraghavan VP, Sirasanagandla SR. Neuroendocrine-associated epigenetic factors in cellular senescence: mechanisms and therapeutic implications. Biogerontology. 2026; 27(2): 64.
[20] Ponnusamy B, Rajagopal P, Palanisamy CP, Veeraraghavan VP, Jayaraman S. Mechanistic Exploration of the anticancer activity of Justicia adhatoda Plant Leaf Ethanolic Extract against Colon Cancer Cells: An in silico and in vitro Approach. Asian Pacific Journal of Cancer Prevention. 2026; 27(3): 1069-1080.
[21] Pei J, Saran VS, Sivaramakrishnan R, Kanniappan GV, Pandurangan V, Jayaraman S, Dhayalan VK, Mironescu M, Mironescu ID, Palanisamy CP. Ultrasonic-assisted, Sargassum ilicifolium (brown marine macroalgae)-mediated biogenic synthesis of CuO nanoparticles incorporated in starch/PVA electrospun nanoscaffolds: In vitro safety and antioxidant efficacy assessment. Bioorganic Chemistry. 2026; 173: 109679.
[22] Raj MAPA, Subramaniyam S, Kanniappan GV, Jayaraman S, Palanisamy CP. Sustainable fabrication of starch/PVA/CuO electrospun nanoscaffolds from Turbinaria ornata (marine macroalgae) extract: Physicochemical characterization and antidiabetic evaluation. Kuwait Journal of Science. 2026; 53(2): 100545.
[23] Pei J, Ganesh NS, Subramaniyam S, Sivaramakrishnan R, Kanniappan GV, Jayaraman S, Palanisamy CP. Sustainable fabrication of starch/PVA/CuO electrospun nanoscaffolds from Padina tetrastromatica (Brown macroalgae) extract: Physicochemical characterization and antidiabetic assessment. Sustainable Chemistry One World. 2026; 9: 100195.
[24] Sakthiraj A, Sivaramakrishnan R, Subramaniyam S, Kanniappan GV, Pandurangan V, Jayaraman S, Dhayalan VK, Mironescu M, Mironescu ID, Palanisamy CP. Starch/PVA electrospun nanoscaffolds loaded with ultrasonic-assisted green-synthesis of CuO nanoparticles from marine macroalgae (Gracilaria corticata) extract: Cytotoxicity and antioxidant analysis. Chemical Physics Impact. 2026; 12: 101018.
[25] Raju M, Chandrasekaran MK, Loganathan L, Ahalliya RM, Mironescu M, Mironescu ID, Palanisamy CP, Kanniappan GV. Lipid remodeling and ferroptosis in phosphatidylcholine-mediated tumor–stroma crosstalk. Frontiers in Molecular Biosciences. 2026; 13: 1742305.

[26] Kunamalla R, Panagal M, Palanisamy CP. Biogenic synthesis and fabrication of starch/PVA/CuO electrospun nanoscaffolds from Sargassum ilicifolium (brown marine macroalgae) extract for anticancer activity on HT-29 and MCF-7 cancer cells. Biocatalysis and Agricultural Biotechnology. 2026; 72: 103923.
[27] Pei J, Govindaraj H, Sivaramakrishnan R, Kanniappan GV, Pandurangan V, Dhayalan VK, Mironescu M, Mironescu ID, Jayaraman S, Palanisamy PC. Sustainable fabrication of biopolymer-based (starch/PVA) nanoscaffolds loaded with green-synthesized CuO nanoparticles from Sargassum wightii (marine macroalgae): Cytocompatibility and antioxidant activity. Biomaterials Advances. 2026; 182: 214660.
[28] Pei J, Perumal NC, Meng P, Long Q, Palanisamy CP. Extracellular vesicle-based biosensors for Alzheimer's disease: A new frontier in precision diagnostics. Ageing Research Reviews. 2026; 113: 102904.
[29] Shree P, Sivaramakrishnan R, Kanniappan GV, Pandurangan V, Jayaraman S, Dhayalan VK, Mironescu M, Mironescu ID, Palanisamy CP. Antioxidant and biocompatible CuO-starch/PVA nanoscaffolds via ultrasonic green synthesis using Turbinaria conoides (brown marine macroalgae). Medicine in Drug Discovery. 2025; 28: 100238.
[30] Gong J, Lin J, Guan T, Pei J, Palanisamy CP, El-AtyFrom AMA. selenium tolerance to nanoplastic antagonism: Comprehensive characterization of L. casei SNUT1 and its extracellular vesicle–nanoselenium complex. Food Bioscience. 2025; 74: 107749.
[31] Poochi SP, Sundarraj R, Raju MV, Chandrasekaran MK, Ahalliya RM, Palanisamy CP, Kanniappan GV, Kondapavuluri BK, Thiruvengadam M. Harnessing Nature: Computational and Experimental Insights Into *Ipomoea obscura* Metabolites for Bladder Cancer Therapy. Chemistry and Biodiversity. 2025; 0: e00909.
[32] Dugganaboyana GK, Kannankumar MKG, Shivaramakrishna S, Raju MV, Chandrasekaran MK, Ahalliya RM, Panneerselvam N, Palanisamy CP, Kanniappan GV. Phytochemical insights, antioxidant activity and therapeutic potential of Cassia senna against prostate cancer in Wistar albino rats. Discover Applied Sciences. 2025; 7:1206.
[33] Natarajan SR, Krishnamoorthy R, Alshuniaber MA, Gatasheh MK, Rajagopal P, Veeraraghavan VP, Palanisamy CP, Jayaraman S. KDM1A Facilitates Oncogenic Potential in Colorectal Cancer Progression Through the Activation of AXIN/GSK3β/β-Catenin Signaling Pathways: Evidence From Integrated Transcriptomics and In Vitro Studies. The Journal of Gene Medicine. 2025; 27(11): e70053.
[34] Guan T, Gong J, Lin J, Palanisamy CP, Jinjin Pei J, El-Aty AMA. Machine learning-driven multimodal optimization of selenium biotransformation and flavor profiling in fermented apple–Yacon functional beverages. Innovative Food Science & Emerging Technologies. 2025; 105: 104198.
[35] Natarajan SR, Krishnamoorthy R, Alshuniaber MA, Alsulami TS, Gatasheh MK, Rajagopal P, Palanisamy CP, Govindan R, Veeraraghavan VP, Jayaraman S. ABCE1 facilitates tumour progression via aerobic glycolysis and inhibits cell death in human colorectal cancer cells through the p53 signalling pathway. Scientific Reports. 2025; 15: 24674.
[36] Huang Y, Guo H, Liu Y, Jin W, Palanisamy CP, Pei J, Oz F, El-Aty AMA. Effects of Natural Polysaccharides on the Gut Microbiota Related to Human Metabolic Health. Molecular Nutrition & Food Research. 2025; 69:e202400792.
[37] Poornima K, Meenakshi K.C, Manikandan V.R, Shankari G, Prabhu D, Rathi M.A, Palanisamy CP, Balaji R, Gopalakrishnan V.K. Exploring the anticancer potential of Jerantinine A from *Tabernaemontana coronaria* against prostate, breast, and ovarian cancers: A computational approach. *Journal of Complementary and Integrative Medicine*, 2025 22(2): 363–372.
[38] Palanisamy CP, Poompradub S, Sansanaphongpricha K, Jayaraman S, Subramani K. Faridah Sonsudin gGreen synthesis of Nigella sativa-mediated silver nanoparticles for enhanced antibacterial activity and wound healing: Mechanistic insights and biomedical applications. Environmental Nanotechnology, Monitoring & Management. 2025; 24: 101085.
[39] Surendran N, Raju MV, Chandrasekaran MK, Ahalliya RM, Palanisamy CP, Chandrasekaran G, Kanniappan GV. Physicochemical characterization of starch from Maranta arundinacea L.(arrowroot) rhizomes and its inhibition of COX-2: In vivo validation. Bioactive Carbohydrates and Dietary Fibre. 2025; 33: 100465.
[40] Kannappan P, Chandrasekaran MK, Raju MV, Gopalakrishnan S, Dhamodharan P, Ahalliya RM, Palanisamy CP, Raju B, Kanniappan GV. Exploring the anticancer potential of Jerantinine A from Tabernaemontana coronaria against prostate, breast, and ovarian cancers: a computational approach. Journal of Complementary and Integrative Medicine. 2025; 22(02): 363-372.
[41] Pei J, Kumarasamy RV, Jayaraman S, Kanniappan GV, Long Q, Palanisamy CP. Quercetin-functionalized nanomaterials: Innovative therapeutic avenues for Alzheimer's disease management. Ageing Research Reviews. 2025; 104: 102665.
[42] Jayaraman S, Prasad M, Natarajan SR, Krishnamoorthy R, Alshuniaber MA, Gatasheh MK, Veeraraghavan VP, Rajagopal P, Palanisamy CP. Molecular mechanisms underlying the effects of beta-sitosterol on TGF-β1/Nrf2/SIRT1/p53-mediated signaling in the kidney of a high-fat diet and sucrose-induced type-2 diabetic rat. Chemico-Biological Interactions. 2025; 411: 111443.
[43] Huang Y, Guo H, Liu Y, Jin W, Palanisamy CP, Pei J, Oz F, El-Aty AMA. Effects of Natural Polysaccharides on the Gut Microbiota Related to Human Metabolic Health. Molecular Nutrition & Food Research. 2025; e202400792.

[44] Prabhakaran P, Palanisamy CP, Shanmugam A, Damodharan P, Swaminathan H, Devaraj D, Ahalliya RM, Kanniappan GV. Isolation, structural characterization, and molecular docking studies on the bioactive compound from n-Hexane extract of Emilia sonchifolia (L.) DC against the pancreatic cancer target Aurora 2 Kinase. Journal of Complementary and Integrative Medicine. 2024; 22(1): 0290.
[45] Jiang H, Kumarasamy RV, Pei J, Raju K, Kanniappan GV, Palanisamy CP. Integrating engineered nanomaterials with extracellular vesicles: Advancing targeted drug delivery and biomedical applications. Frontiers in Nanotechnology. 2024; 6: 1513683.
[46] Guo H, Liu Y, Wan T, Song D, Palanisamy CP, Geng J, Pei J, Özmen S, El-Aty AMA. Toward personalized cancer management: Role of precision nutrition–diet interventions. Journal of Functional Foods. 2024; 123: 106584.
[47] Natarajan SR, Krishnamoorthy R, Alshuniaber MA, Al-Anazi KM, Farah MA, Rajagopal P, Palanisamy CP, Veeraraghavan VP, Jayaraman S. Identification of FOXM1 as a novel protein biomarker and therapeutic target for colorectal cancer progression: Evidence from immune infiltration and bioinformatic analyses. International Journal of Biological Macromolecules. 282 (Part 4): 137201.
[48] Rajendran MS, Jayaraman S, Khan JM, Jasmine S, Prabhakaran RK, Raju MV, Chandrasekaran MK, Ahalliya RM, Kannappan P, Palanisamy CP, Kanniappan GV. Investigating the colon toxicity and carcinogenic role of monosodium glutamate compared with Dimethylhydrazine in male Wistar rats: Exploring the link to childhood colon cancer risk. Journal of King Saud University - Science. 2024; 36(11): 103507.
[49] Kumarasamy RV, Natarajan P, Umapathy VR, Roy JR, Rab SO, Saeed M, Panagal M, Mironescu M, Srinivasan GP, Palanisamy CP. Clinical Applications and Therapeutic Potentials of Advanced Nanoparticles: A Comprehensive Review on Completed Human Clinical Trials. Frontiers in Nanotechnology. 2024; 6:1479993.
[50] Natarajan PM, Umapathy VR, Murali A, Swamikannu B. (2022). Computational Simulations of Identified marine-derived Natural Bioactive Compounds As Potential Inhibitors of Oral Cancer. Future Science OA. 2022; 8(3).
[51] Natarajan PM, Umapathy VR. Role of transcriptomics in the study of oral cancer. Frontiers in Oral Health. 2025; 6:1524364.
[52] Vidhyarekha U, Natarajan PM, Bhuminathan S, Sabarinathan J, Suba R, Vijayalakshmi P. Role of artificial intelligence in Oral Cancer. Advances in Public Health. 2024. 2024: 3664408.
[53] Ganesan A, Kumar NG, Natarajan PM, Gauthaman J. Automated classification of elongated styloid processes using deep learning models-an artificial intelligence diagnostics. Frontiers in Oral Health. 2025; 5: 1424840.
[54] Umapathy VR, Natarajan PM, Swamikannu B. Regenerative Strategies in Dentistry: Harnessing Stem Cells, Biomaterials and Bioactive Materials for Tissue Repair. Biomolecules. 2025; 15: 546.
[55] Natarajan PM. Dental Bioinformnatics-Current Scope and Future perspectives. Research Journal of Pharmacy and Technology. 2022;15(5):2351-6.
[56] Ganesan A, Kumar NG, Natarajan PM. Solanum trilobatum leaf extract-derived silver nanoparticles downregulate the PI3K/AKT/mTOR signaling pathway and attenuate oral squamous cell carcinoma cell proliferation. Journal of Herbmed Pharmacology. 2024; 13(2): 300-307.
[57] Perumal MKK, Renuka RR, Subbiah SK, Natarajan PM. Artificial intelligence-driven clinical decision support systems for early detection and precision therapy in oral cancer: a mini review. Frontiers in Oral Health. 2025; 6: 1592428.
[58] Ramesh E, Ganesan A, Lakshmi KC, Natarajan PM. Artificial intelligence-based diagnosis of oral leukoplakia using deep convolutional neural networks Xception and MobileNet-v2. Frontiers in Oral Health. 2025; 6: 1414524.
[59] Ganesan A, Kumar NG, Natarajan PM. Anticancer activity of silver nanoparticles synthesized from aqueous leaf extract of Solanum trilobatum (Purple fruit pea eggplant) on human oral cancer cells. Journal of Herbmed Pharmacololgy. 2024; 13(2): 260-268.
[60] Jin W, Pei JJ, Roy JR, Jayaraman S, Ahalliya RM, Kanniappan GV, Mironescu M, Palanisamy CP. Comprehensive review on single-cell RNA sequencing: A new frontier in Alzheimer's disease research. Ageing Research Reviews. 2024; 274: 102454.
[61] Pei J, Palanisamy CP, Jayaraman S, Natarajan PM, Umapathy VR, Roy JR, Panagal M, Jayaraman S. Curcumin-loaded polymeric nanomaterials as a novel therapeutic strategy for Alzheimer's disease: A comprehensive review. Ageing Research Reviews. 2024; 99: 102393.
[62] Pei J, Palanisamy CP, Jayaraman S, Natarajan PM, Umapathy VR, Roy JR, Thalamati D, Ahalliya RM, Kanniappan GV, Mironescu M. A comprehensive review on starch-based Sustainable Edible Films Loaded with Bioactive Components for Food Packaging. International Journal of Biological macromolecules. 2024; 274 (Part-1): 133332.
[63] Palanisamy CP, poompradub S, Sansanaphongpricha K, Subramani K, Sonsudin F. Increased expression levels of PDGF and VEGF magnify the wound healing potential facilitated by biogenic synthesis of silver nanoparticles. Nano-Structures & Nano-Objects. 2024; 39: 101236.
[64] Pei J, Palanisamy CP, Jayaraman S, Natarajan PM, Umapathy VR, Roy JR, Thalamati D, Ahalliya RM, Kanniappan GV, Mironescu M. Proteomics Profiling of Extracellular Vesicle for Identification of Potential Biomarkers in Alzheimer's Disease: A Comprehensive Review. Ageing Research Reviews. 2024; 99: 102359.

[65] Xi J, Wang T, Xian P, Liu X, Du M, Yang H, Palanisamy CP, Lin W, Long Q. Proteomic insights uncover enhanced neurotherapeutic potential in conditioned mesenchymal stem cell-derived extracellular vesicles. Extracellular Vesicle. 2024; 3: 100037.
[66] Pei J, Natarajan PM, Umapathy VR, Swamikannu B, Sivaraman NM, Krishnasamy L, Palanisamy CP. Advancements in the synthesis and functionalization of zinc oxide-based nanomaterials for enhanced oral cancer therapy. Molecules. 2024; 29(11): 2706.
[67] Gatasheh MK, Natarajan SR, Krishnamoorthy R, Alsulami TS, Rajagopal P, Palanisamy CP, Veeraraghavan VP, Jayaraman S. Molecular analysis to identify novel potential biomarkers as drug targets in colorectal cancer therapy: an integrated bioinformatics analysis. Molecular and Cellular Oncology. 2024; 11(1): 2326699.
[68] Pei J, Yan Y, Jayaraman S, Rajagopal P, Natarajan PM, Umapathy VR, Gopathy S, Roy JR, Sadagopan CS, Thalamati D, Palanisamy CP, Mironescu M. A review on advancements in the application of starch-based nanomaterials in biomedicine: Precision drug delivery and cancer therapy. International Journal of Biological Macromolecules. 2024; 130746.
[69] Pei JJ, Yan Y, Palanisamy CP, Jayaraman S, Natarajan PM, Umapathy VR, Gopathy S, Roy JR, Sadagopan JC, Thalamati D, Mironescu M. Materials-based drug delivery approaches: Recent advances and future perspectives. Green Processing and Synthesis. 2024; 13: 20230094.
[70] Pei JJ, Deng W, Liu Y, Guo Y, Chen J, Abdu H, Khan MR, Palanisamy CP, El-Aty AM. A Comprehensive Review of Cornus officinalis: Health Benefits, Phytochemistry, and Pharmacological Effects for Functional Drug and Food Development. Frontiers in Nutrition. 2023; 10: 1309963.
[71] Alugoju P, Palanisamy CP, Anthikapalli NVA, Jayaraman S, Prasanskulab A, Chuchawankul S, Dyavaiah M, Tencomnao T. Exploring the anti-aging potential of natural products and plant extracts in budding yeast Saccharomyces cerevisiae: A review. F1000Research. 2023; 12: 1265.
[72] Lavanya M, Krishnamoorthy R, Alshuniaber MA, Manoharadas S, Palanisamy CP, Veeraraghavan VP, Jayaraman S, Rajagopal P, Padmini R. Formulation, characterization and evaluation of gelatin-syringic acid/zinc oxide nanocomposite for its effective anticancer, antioxidant and anti-inflammatory activities. Journal of King Saud University-Science. 2023; 35: 102909.
[73] Palanisamy CP, Poompradub S, Sansanaphongpricha K, Jayaraman S, Subramani K, Sonsudin F. Biosynthesis of silver nanoparticles (AgNPs) using ethanolic extract of Nigella sativa (L.) seeds promotes wound healing via PDGF and VEGF signalling pathways activation. Biocatalysis and Agricultural Biotechnology. 2023; 54: 102970.
[74] Prasad M, Jayaraman S, Natarajan SR, Veeraraghavan VP, Krishnamoorthy R, Gatasheh MK, Palanisamy CP, Elrobh M. Piperine modulates IR/Akt/GLUT4 pathways to mitigate insulin resistance: Evidence from animal and computational studies. International Journal of Biological Macromolecules. 2023; 253: 127242.
[75] Palanisamy CP, Pei JJ, Phaniendra A, Venkata AAN, Jayaraman S, Veeraragahavan VP, Sridevi G, Roy JR, Janaki CS, Thalamati D, Mironescu M, Luo Q, Chai Y, Long Q. New Strategy of Neurodegenerative Disease Treatment with Extracellular Vesicles (EVs) Derived from Mesenchymal Stem Cells (MSCs). *Theranostics*. 2023; 13(12):4138-4165. doi:10.7150/thno.83066.
[76] Palanisamy CP, Phaniendra A, Jayaraman S, Poompradub S. *Nigella sativa* L. seed extracts promotes wound healing progress by activating VEGF and PDGF signalling pathways: *An in vitro* and *in silico* study. *F1000 Research*. 2023; 12: 436.
[77] Pei JJ, Palanisamy CP, Phaniendra A, Venkata AAN, Natarajan PM, Umapathy VR, Swamikannu B, Jayaraman S, Rajagopal P, Poompradub S. A comprehensive review on bio-based materials for chronic diabetic wounds. *Molecules*. 2022; 28(2), 604.
[78] Palanisamy CP, Cui B, Zhang H, Gunasekaran VP, Ariyo A, Jayaraman S, Veeraraghavan V, Rajagopal P. A critical review on starch-based electrospun nanofibrous scaffolds for wound healing application. International Journal of Biological Macromolecules. 2022; 222 (Part: B): 1852-1860.
[79] Monisha P, Ponnulakshmi R, Nalini D, Vishnu P V, Palanisamy CP, Cui B, Shankargouda P, Selvaraj J. A comprehensive review on high fat diet-induced diabetes mellitus: An epigenetic view. The Journal of Nutritional Biochemistry. 2022; 2022: 109037.
[80] Monisha P, Selvaraj J, Mohamed AE, Mohamed E, Mosaab AEA, Vishnu PV, Srinivasan V, Vidhya RU, Shazia FJH, Kalaiselvi K, Durairaj S, Palanisamy CP, Surapaneni K M, Ponnulakshmi R. A Comprehensive review on therapeutic perspectives of phytosterols in insulin resistance: A mechanistic approach. Molecules. 2022; 27(5): 1595.